COMSOL Simulation of a Dual-axis MEMS Accelerometer with T-shape Beams

Leonardo Bove
Dipartimento di Ingegneria dell'Informazione
University of Pisa
l.bove3@studenti.unipi.it

***Abstract*—This paper presents the mechanical response of a MEMS dual-axis accelerometer with T-shaped beams for different values of X and Y axes accelerations. The original design idea and simulation are taken from an excerpt from the *Proceedings of the 2015 COMSOL* Conference in Boston [2]. The aim of this paper is to validate the results obtained in the reference through a COMSOL 6.0 Multiphysics simulation. The results show the inertial mass displacement and the induced stress. Beams equivalent elastic constants and displacement sensitivities to accelerations (S_x, S_y) along X and Y axes were evaluated and compared to theoretical forecasts. Accelerations up to 50g were simulated. Moreover, the dependence of the sensitivity along the X axis was evaluated for different values of the spring arms' dimensions w_{bx} and t_{bx}. The obtained results are compared with the theoretical models proposed in the referenced paper.**

I. Introduction

NOWADAYS, MEMS accelerometers have an extensive applications range: consumer electronics, automotive systems, aerospace, and robotics. Small size, together with low power consumption and cost-effectiveness, turn them into the basis in inertial navigation and motion sensing. One critical evolution in the technology for MEMS accelerometers involves the development of dual-axis devices that can measure accelerations along two orthogonal axes in a single package. These designs improve integration efficiency and reduce the complexity of aligning several single-axis accelerometers.

This report focuses on the analysis and optimization of a MEMS dual-axis accelerometer featuring T-shaped beams. The special geometry of these beams allows for the measurement of accelerations along both the X and Y axes through differential capacitance sensing. Theoretical basics of the accelerometer design, as mentioned in the referred article, are modeled and simulated in COMSOL Multiphysics.

The main objectives of this study are:

- Calculating the displacement of the inertial mass and the induced stress for several acceleration inputs along both the X and Y axes. The range of accelerations is the same as the one simulated in the original paper, i.e. up to 50g in both directions.
- Obtaining the equivalent elastic constants of the beams and the device displacement sensitivity to accelerations, S_x and S_y, in both axes.
- Carrying out a parametric analysis to study the dependence of sensitivity, S_{dx}, on the spring arm dimensions w_{bx} and t_{bx}.
- Comparing simulation results with theoretical predictions in order to validate the model and identify areas for possible design improvements.

II. Structure Design and Analysis

The structure of the analysed device is shown in figure 1. This accelerometer is designed to be fabricated with polysilicon surface-micromachining. The whole device is symmetric vertically and horizontally: these symmetries will be exploited later to reduce the COMSOL model size.

The central movable mass is anchored through two T-shape beams. Each T-shape beam consists of one straight beam and two folded beams.

Attached to the central mass, there are 64 movable fingers, divided into 8 groups. Each side of the central mass has 2 groups of fingers. Each of them faces one fixed finger and the capacitance between those is used to sense the external acceleration. The vertical fingers (aligned along the Y axis) together with the straight beams are used to sense acceleration along X direction, so they are called X-beams and X-capacitance groups. On the other hand, the horizontal fingers (aligned along the X axis) together with the folded beams are used to sense acceleration along Y direction, so they are called Y-beams and Y-capacitance groups. Due to the symmetry of the device, two of the four groups of X movable fingers have fixed fingers on the left side, whereas the other two groups have them on the right. Similarly, this apply to Y-movable fingers groups: two of them have fixed fingers in the upper side, the other two on the down side. This is helpful for obtaining a differential capacitance, as will be explained in section II-B3.

A. Device Geometrical Sizing

A detailed view of the geometrical model used in this COMSOL simulation is presented in figure 2. As anticipated, in order to reduce the size of the model, only $\frac{1}{8}$ of the whole device was simulated, taking advantage of the symmetries along X, Y and Z axes.

Table I shows all the geometrical parameters of the device, which are identical to those used in [2]. The only dimensions that were missing are those of the folded beams junction element.

The whole geometrical description of the device was parametrized on COMSOL, in order to make it more flexible

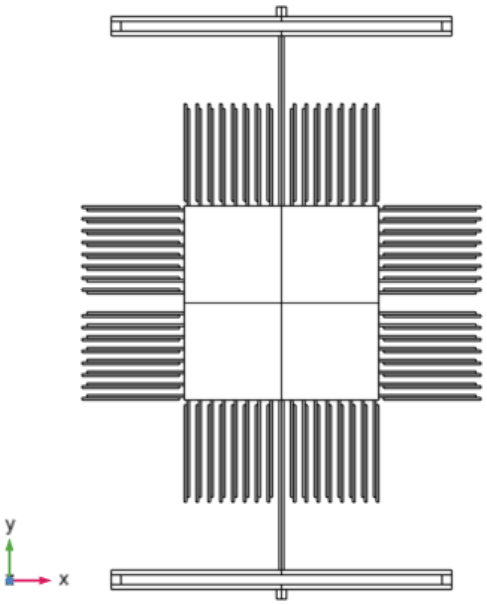

Fig. 1. Device structure.

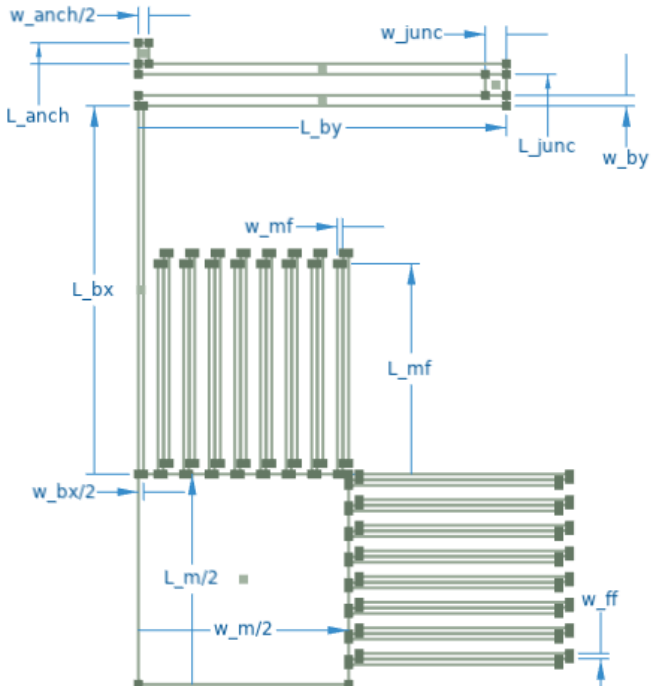

Fig. 2. Device dimensions.

and allow for geometrical parametric sweeps. The parameters labels used, as shown in figure 2, are the following:

- L_m, w_m, t_m: length, width and thickness of the central mass.
- L_{bx}, w_{bx}, t_{bx}: length, width and thickness of the straight X beam.
- L_{by}, w_{by}, t_{by}: length, width and thickness of the folded Y beams segments.
- L_{junc}, w_{junc}: length and width of the folded Y beams junctions. The thickness is the same as the other segments.
- L_{anch}, w_{anch}: length and width of the anchor. The thickness is the same as the folded beams.
- L_{mf}, w_{mf}, t_{mf}: length, width and thickness of the movable fingers.
- L_{ff}, w_{ff}: length and width of the fixed fingers. The thickness is the same as the movable fingers.

TABLE I
DEVICE COMPONENTS DIMENSIONS

Components	Quantity	Length (μm)	Width (μm)
Central mass	1	800	800
Movable fingers	64	400	10
Fixed fingers	64	400	10
Folded beam segments	8	700	20
Folded beam junctions	4	40	40
Straight beams	2	700	20
Anchors	2	40	40

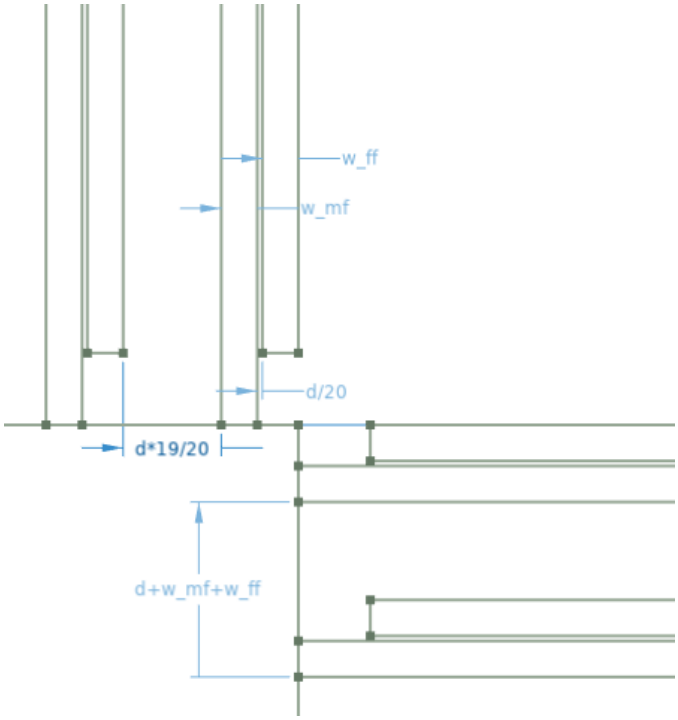

Fig. 3. Fixed fingers alignment detail.

The 8 fixed fingers at the vertices of the central mass are assumed to be aligned with the side of the mass itself, as shown in figure 3.

The fingers of each group are assumed to be equally spaced and this spacing is the same for both the vertical and the horizontal groups. This spacing is parametrically defined from the available space for the movable fingers in the upper mass side, where the width of the straight beam must be taken into account. The free space between each fixed finger d is defined

as follows:

$$d = \frac{\frac{L_m}{2} - 8 * (w_{mf} + w_{ff}) - \frac{w_{bx}}{2}}{8} = \quad (1)$$

Therefore, the pitch of the fixed (movable) fingers is equivalent to:

$$pitch = d + w_{mf} + w_{ff} \quad (2)$$

The distance between each movable finger and its adjacent fixed fingers is not the same: as we can see from figure 3, in the upper-right side of the device the vertical movable fingers are positioned so that the fixed finger on the right is at distance $\frac{d}{20} = 1.4375\mu m$, whereas the one on the left is at distance $d - \frac{d}{20} = 27.3125\mu m$, which is much larger than the first one; on the other hand, thanks to the symmetry, the vertical movable fingers of the upper-left side are much closer the the fixed fingers on their left. Similarly, the same arrangement is used for the horizontal fingers, which are symmetric between the top and bottom sides. This will be helpful for the measurement of the differential capacitance, see section II-B3.

Also the overlapping between the movable and fixed fingers had to be assumed and it was parametrically defined for both the vertical ($L_{ov,v}$) and horizontal ($L_{ov,h}$) fingers and set to $L_{ov,v} = L_{ov,h} = 380\mu m$.

The outer air box that contains the device was defined to be larger than the maximum dimensions of the accelerometer by an offset of $box_{offset} = 50\mu m$. This is true for every side of the accelerometer, except for the three symmetry planes.

B. Theoretical Analysis

We now discuss the mathematical models used to predict the behaviour of this system.

1) Beams Stiffness: The simplified mechanical model of the system is presented in figure 4.

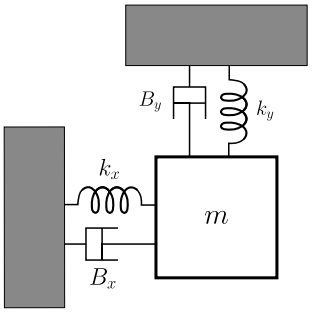

Fig. 4. Simplified mechanical model of the dual axis accelerometer.

Here, k_x and k_y are the **equivalent stiffness constants** of the springs that allow, respectively, displacements along the X axis and the Y axis; B_x and B_y are the equivalent damping constants along the two axis, but they are not relevant in this study, given that we are evaluating the steady state of the system; m is the total inertial mass, i.e. the mass of the central block and of the movable fingers. m is given by the following equation:

$$m = \rho_{poly} \cdot (w_m l_m t_m + 64 \cdot w_{mf} l_{mf} t_{mf}) \quad (3)$$

where we neglect the mass of the beams. If we now assume that all the displacement along the X axis is due to the bending of the two straight beams and that the displacement along the Y axis is due to deformation of the two folded beams, we can say that k_x is equal to the equivalent spring constant of the straight beams combined and k_y is the one of the folded beams. We will also assume that there is no cross stiffness constant, i.e. we can neglect any displacement along the X axis due to forces along the Y axis and vice versa.

Given these hypothesis, we can model the straight beam to be rigidly attached to the end of the folded beam (which we supposed to be fixed for X accelerations) and to have a roller, i.e. a guided end, on the other side, due to the infinitely rigid central mass, as shown in figure 5. We suppose that all the force due to the acceleration of the inertial mass is concentrated at the right end of the beam.

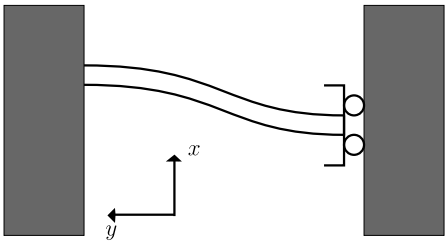

Fig. 5. Straight beam model. On the right there is the central mass.

The equivalent stiffness constant of this type of structure, due to a force along the X axis concentrated at the right end, is well known in the scientific literature and is given by the following equation:

$$k_{straight} = 12\frac{EJ}{L^3} \quad (4)$$

where E is the Young's modulus of the polysilicon, L is the length of the beam and J is the moment of inertia of the beam's section, due to a bending moment along the z axis (see the reference plane used in figure 5). In our case:

$$J = \frac{bh^3}{12} = \frac{t_{bx} w_{bx}^3}{12} \quad (5)$$

Hence, the equivalent stiffness of one straight beam is

$$k_{straight,x} = \frac{E t_{bx} w_{bx}^3}{L_{bx}^3} \quad (6)$$

Given that the two straight beams undergo the same displacement, thanks to the symmetry of the model, we can easily consider the two springs in parallel and the total x stiffness will be given by the sum of the two spring constants:

$$k_x = 2 \cdot k_{straight,x} = 2\frac{E t_{bx} w_{bx}^3}{L_{bx}^3} = 31.5335 N/m \quad (7)$$

For what concerns the stiffness along the Y axis, we can model the two segments of the folded beam as in figure 5, therefore each segment has the same stiffness as the straight beam, taking into account the different geometrical dimensions.

$$k_{straight,y} = \frac{Et_{by}w_{by}^3}{L_{by}^3} \tag{8}$$

The two segments are attached one to the other through the junction segment, which is supposed to be infinitely rigid and not to be able to bend, due to its aspect ratio. For this reason we can model it as a roller. Given that the two segment are mechanically in series and they have the same spring constant, the total stiffness is half of a single one:

$$k_{folded} = \frac{k_{straight,y} \cdot k_{straight,y}}{k_{straight,y} + k_{straight,y}} = \frac{k_{straight,y}}{2} \tag{9}$$

Now, given that for each T beam there are two folded beams and that all of them undergo the same displacement (as absolute value), we can model these four springs as if they were in parallel and the total y stiffness is given by the following equation:

$$k_y = 4 \cdot k_{folded} = 4\frac{k_{straight,y}}{2} = 2\frac{Et_{by}w_{by}^3}{L_{by}^3} = 31.5335N/m \tag{10}$$

However, we need to keep in mind that the COMSOL model will be only $\frac{1}{8}$ of the total model, as explained in section II-A. Therefore, the spring dimensions will be different and the inertial mass will be $\frac{1}{8}$ of the total inertial mass. We can find an analytical relationships between the reduced spring constants and the complete ones, so that we can compare the output of the simulation with the theoretical model.

Thanks to the symmetry of the model, we can affirm that the stiffness of the reduced springs will be $\frac{1}{8}$ of the total corresponding springs, because it is possible to see all the reduced springs as if they were in parallel to each other.

$$k_{x,reduced} = \frac{k_x}{8} \tag{11}$$

$$k_{y,reduced} = \frac{k_y}{8} \tag{12}$$

This coefficients will be multiplied by the spring constants found in simulation.

2) Displacement Sensitivity To Accelerations: The **displacement sensitivity** is defined as the displacement of the movable fingers when $1g$ of acceleration is applied. Therefore, considering the equivalent mechanical model of the system, we can evaluate the sensitivity along the two axes. Since we neglected the cross stiffness, the displacement is given by the following equations:

$$\Delta x = \frac{F_x}{k_x} \tag{13}$$

$$\Delta y = \frac{F_y}{k_y} \tag{14}$$

where F_x and F_y are the equivalent forces along the respective axis, due to an acceleration of the inertial mass. Hence, the sensitivities:

$$\begin{aligned} S_x = \Delta x|_{a_x=1g,a_y=0} &= \left.\frac{ma_x}{k_x}\right|_{a_x=1g,a_y=0} \\ &= \frac{\rho_{poly} \cdot (w_m l_m t_m + 64 \cdot w_{mf} l_{mf} t_{mf}) g L_{bx}^3}{2 \cdot Et_{bx}w_{bx}^3} \\ &= 0.002587\mu m \end{aligned} \tag{15}$$

$$\begin{aligned} S_y = \Delta y|_{a_y=1g,a_x=0} &= \left.\frac{ma_y}{k_y}\right|_{a_y=1g,a_x=0} \\ &= \frac{\rho_{poly} \cdot (w_m l_m t_m + 64 \cdot w_{mf} l_{mf} t_{mf}) g L_{by}^3}{2 \cdot Et_{by}w_{by}^3} \\ &= 0.002587\mu m \end{aligned} \tag{16}$$

3) Capacitance Sensing: As anticipated before, thanks to the mirrored position of the fixed fingers relative to the movable fingers (e.g. in the upper-right side fixed fingers are on the right of their respective movable fingers, whereas in the upper-left side the opposite happens) differential capacitance can be measured to sense the displacement of the mass due to inertial force.

Each movable finger will have two equivalent parallel capacitances with the adjacent fixed fingers, if the fixed fingers are set at the same voltage. However, as shown in figure 3, the capacitance with the nearest fixed finger is much greater than the other, which can therefore be neglected.

When there is no acceleration, the capacitance gap between each movable finger and its nearest fixed finger is the same and equal to $d_0 = \frac{d}{20}$, therefore the differential capacitance between the left/right (top/bottom) X (Y) capacitance groups is zero.

When a positive X axis acceleration is applied, due to inertial force, the movable fingers move towards right by a displacement x: the right capacitance gap is now $d_r = d_0 - x$, whereas the left capacitance gap is $d_l = d_0 + x$ (see figure 6).

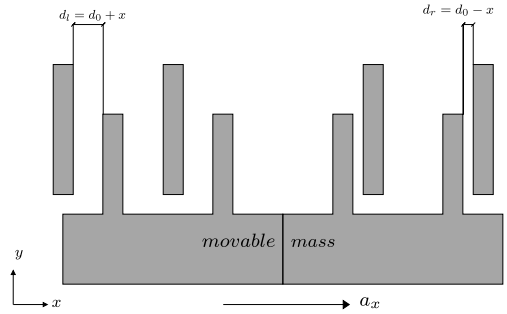

Fig. 6. Capacitance gap variations when an X axis acceleration is applied. Detail of the upper side of the device.

Therefore, we can evaluate the differential X capacitance, defined as the difference between the total right and left groups' capacitances:

$$\Delta C_x = C_r - C_l = 2N_x \left(\frac{\epsilon_0 \epsilon_r S}{d_0 - x} - \frac{\epsilon_0 \epsilon_r S}{d_0 + x}\right) \tag{17}$$

where $S = t_{mf} L_{ov,v}$ is the overlap area between a movable finger and its nearest fixed finger and N_x is the number of

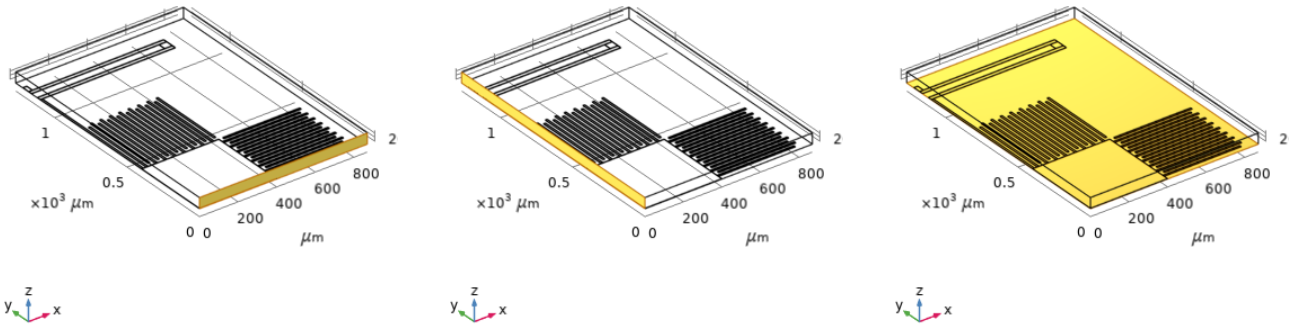

Fig. 7. Symmetry planes, (a) $y = 0$, (b) $x = 0$ and (c) $z = 0$.

movable fingers in a single X capacitance group. This value is doubled, given that there are two right X capacitance groups and two left ones. This expression can be approximated for small displacements:

$$\Delta C_x \cong 4N_x \frac{\epsilon_0 \epsilon_r S}{d_0} \cdot \left(\frac{x}{d_0}\right) \tag{18}$$

Similarly, if we define y as the vertical displacement, the differential horizontal fingers capacitance can be approximated as follows:

$$\Delta C_y \cong 4N_y \frac{\epsilon_0 \epsilon_r S}{d_0} \cdot \left(\frac{y}{d_0}\right) \tag{19}$$

III. COMSOL MULTIPHYSICS

The device was simulated using COMSOL Multiphysics 6.0.

The only COMSOL module used for the simulation of the analysed system is *Solid Mechanics*, because in this study we are not interested in evaluating the capacitance of the device, but only its mechanical properties.

Following [2], the used materials are:

- Air (Built-in)
- Polycrystalline silicon (MEMS)

The polysilicon used is considered to be isotropic, with mass density $\rho_{poly} = 2320 kg/m^3$ and Young's modulus of $E_{poly} = 169 GPa$. The other default material properties are left unchanged.

A. Moving Mesh

The air domain was defined as a **Deforming Domain** in the *Moving Mesh* section. In order to take into account the symmetries of the model, **Symmetry/Roller** were applied on the air domain boundaries, corresponding to the planes $z = 0, y = 0$ and $x = 0$, see 7. However, the Symmetry/Roller forces to zero the displacement of the moving mesh perpendicular to the selected boundary ($\vec{u} \cdot \hat{n} = 0$), therefore, not all these three conditions could be enabled simultaneously. Depending on the type of simulation performed (acceleration along the X axis or Y axis), one of the three symmetry planes becomes, as a matter of fact, an antisymmetry plane and displacements of the moving mesh perpendicular to that plane must be allowed: for example, if an acceleration along X axis is simulated, the Symmetry/Roller associated to the plane $x = 0$ must be disabled.

B. Solid Mechanics

In the *Solid Mechanics* module, similar boundary symmetries were defined: polysilicon boundaries that lay on one of the symmetry planes were included in the **Boundary Symmetry** or **Boundary Antisymmetry** object associated to that plane. Similarly to what was explained before, depending on the current simulation the symmetries and antisymmetries will change: if an X acceleration has to be simulated, the $x = 0$ plane becomes an antisymmetry plane, whereas the $y = 0$ plane is a symmetry plane; the opposite happens for Y acceleration simulations. The plane $z = 0$ will always be a symmetry plane for our studies, given that no accelerations along Z axis will be simulated. All these conditions are already defined inside the *Solid Mechanics* module and they just need to be enabled/disabled. On the bottom boundaries of the fixed fingers and anchor domains, a **Fixed Constraint** condition is applied, as shown in figure 8. This prevents these domains from moving.

All the other domains are set as **Free Linear Elastic Material**. To the *polysilicon* domain, i.e. the whole structure, a **Body Load** was applied. The load was defined as a planar force per unit volume (N/m^3) with components:

$$F_x = a_x g \rho_{poly}$$

$$F_y = a_y g \rho_{poly}$$

$$F_z = 0$$

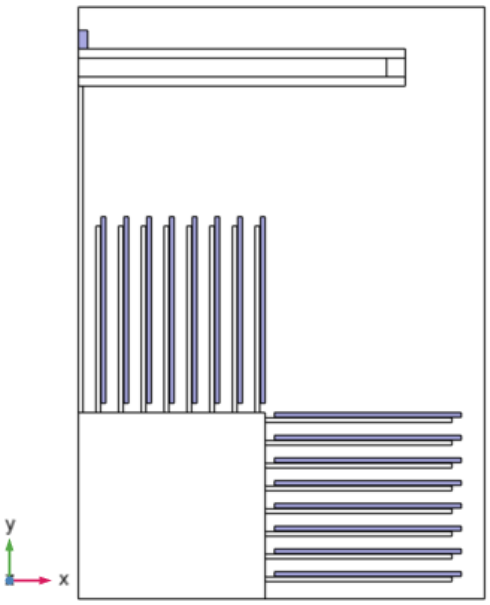

Fig. 8. Fixed boundaries.

where $g = 9.81m/s^2$ is the gravity acceleration, whereas a_x and a_y are two model parameters. These are two pure numbers used to define the external acceleration as a multiple of g.

C. Mesh and Study

The used mesh was of type *physics-controlled* with element size set to **coarse**, in order to follow what done by the authors of [2].

Given that our interest is in the steady state of the system in different conditions, 4 **stationary** studies were defined:

- Parametric sweep of the parameter a_x (X axis acceleration) from $1g$ to $50g$ in 10 steps. a_y is set to 0 and the geometrical parameters are set to their default values, as specified in table I.
- Parametric sweep of the parameter a_y (Y axis acceleration) from $1g$ to $50g$ in 10 steps. a_x is set to 0 and the geometrical parameters are set to their default values, as specified in table I.
- Parametric sweep of the thickness of the straight beam t_{bx} from $1\mu m$ to $30\mu m$ in 20 steps. a_y is set to 0 and a_x is set to $1g$, given that we need to find the displacement sensitivity along the X axis. The other geometrical parameters are set to their default values.
- Parametric sweep of the width of the straight beam w_{bx} from $4\mu m$ to $20\mu m$ in 20 steps. a_y is set to 0 and a_x is set to $1g$, given that we need to find the displacement sensitivity along the X axis. The other geometrical parameters are set to their default values.

In all four studies, the *direct stationary solver* and the *suggested direct solver* were set to **MUMPS**.

IV. Simulation Results

A. a_x parametric sweep

The 3D plots for this simulation are presented in figures 9, 10, 11 and 12.

The maximum displacements along the X axis of the inertial mass are listed in table II.

TABLE II
MAXIMUM X DISPLACEMENT OF THE INERTIAL MASS FOR a_x ACCELERATIONS BETWEEN 1G AND 50G.

a_x [g]	Maximum X displacement [μm]
1.0000	0.0047630
6.4444	0.030692
11.889	0.056615
17.333	0.082532
22.778	0.10844
28.222	0.13435
33.667	0.16025
39.111	0.18614
44.556	0.21202
50.000	0.23790

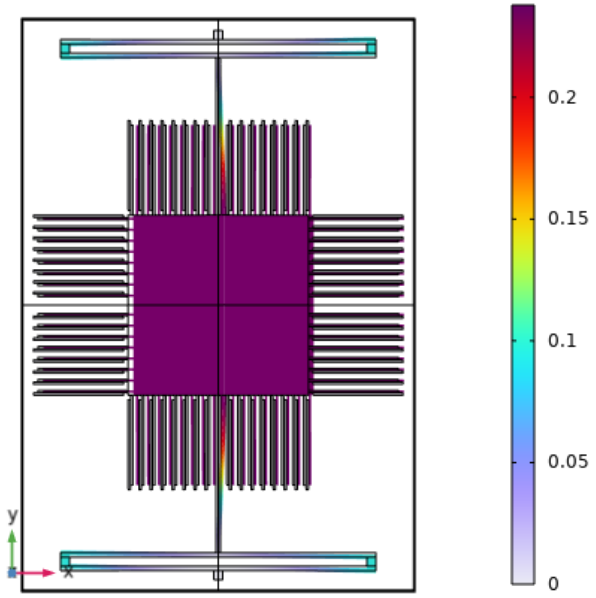

Fig. 9. Displacement (μm) for acceleration $a_x = 50g$.

The maximum von Mises stress evaluated for different accelerations on the polysilicon structure is listed in table III.

The maximum von Mises stress simulated for $a_x = 50g$ is $4.3807 \cdot 10^6 Pa$, which is almost identical to what is obtained in [2] ($4.5594 \cdot 10^6 Pa$). Therefore the conclusions are analogous: according to [1], the minimum fracture strength of polysilicon is $(2.9 \pm 0.5)GPa$ (tensile stress), which is far higher then

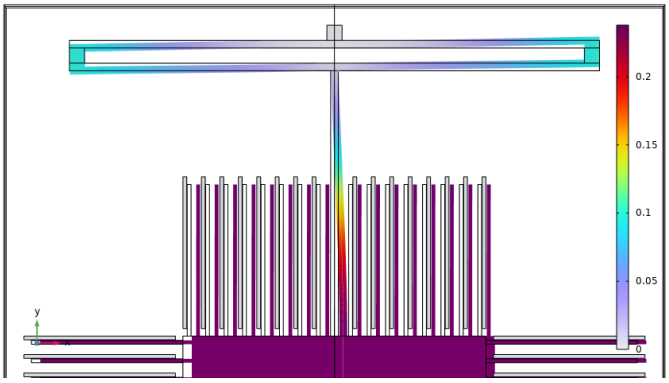

Fig. 10. Displacement (μm) for acceleration $a_x = 50g$, detail.

TABLE III
MAXIMUM VON MISES STRESS OF THE POLYSILICON STRUCTURE FOR a_x ACCELERATIONS BETWEEN 1G AND 50G.

a_x [g]	Maximum Von Mises stress [MPa]
1.0000	0.087655
6.4444	0.56487
11.889	1.0420
17.333	1.5192
22.778	1.9962
28.222	2.4732
33.667	2.9502
39.111	3.4271
44.556	3.9039
50.000	4.3807

what we simulated at $a_x = 50g$, so there are no structural problems at this acceleration.

In figure 13 we can see that the relationship between the x displacement and the x acceleration (therefore, the force) is quite linear, which means that the equivalent x stiffness is constant in the applied range of accelerations, as predicted by our model. The inverse of the mean slope of this curve multiplied by the total simulated inertial mass ($\frac{m}{8}$) gives us an equivalent x stiffness $k_{x,reduced} = 2.1411 N/m$. Using equation 11, we obtain $k_x = 17.1287 N/m$.

As explained in section II-B1, the x displacement sensitivity corresponds to the x displacement of the movable fingers for $a_x = 1g$. Considering the movable fingers as rigid bodies anchored to the central mass, we can evaluate the maximum displacement of the central mass, instead of the fingers'. The obtained sensitivity is $S_x = 0.004763 \mu m$.

TABLE IV
COMPARISON OF SIMULATED AND THEORETICAL VALUES FOR THE X EQUIVALENT STIFFNESS AND S_x SENSITIVITY.

Device Property	COMSOL	Theoretical
k_x [N/m]	17.1287	31.5335
S_x [μm]	0.004763	0.002587

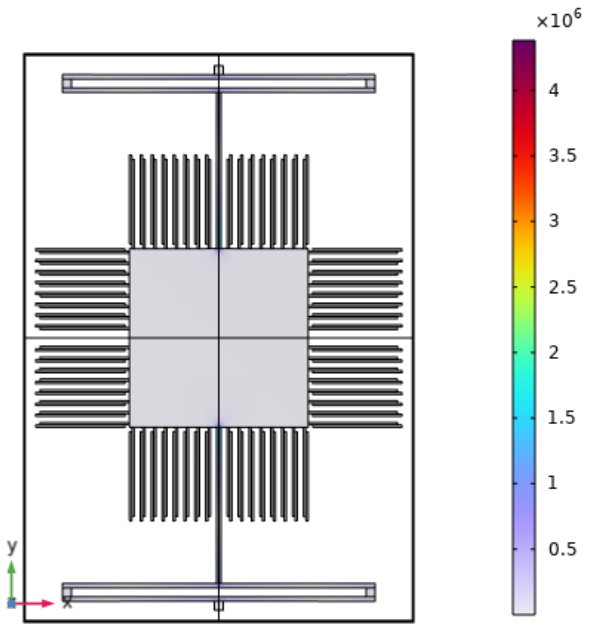

Fig. 11. Von Mises stress intensity (N/m^2) for acceleration $a_x = 50g$.

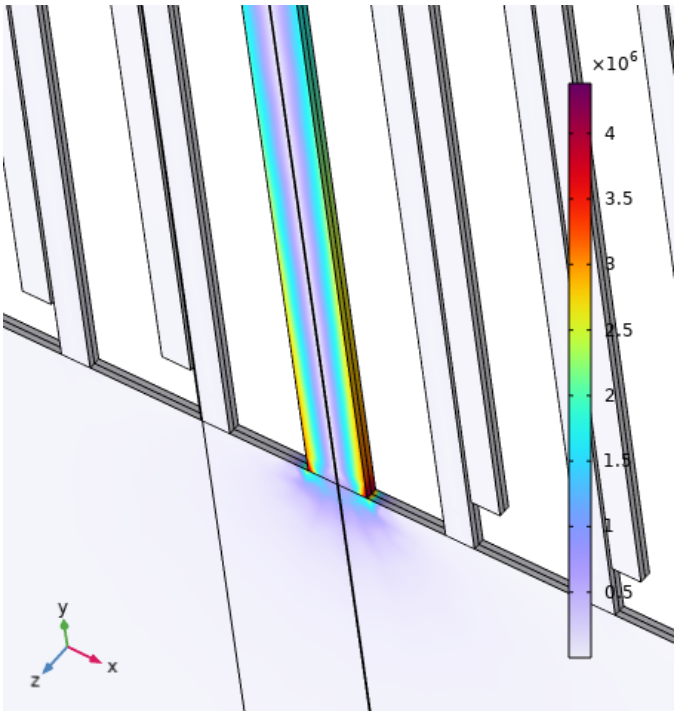

Fig. 12. Von Mises stress intensity (N/m^2) for acceleration $a_x = 50g$, detail of the straight beam attachment to the central mass.

As we can see from this table, the difference with the predicted values is considerable: the simulated value is almost half of the stiffness obtained with our theoretical model. This is reasonable and it is due to the fact that we approximated the folded beam segments as fixed when applying accelerations along the x axis. As it is possible to notice from the

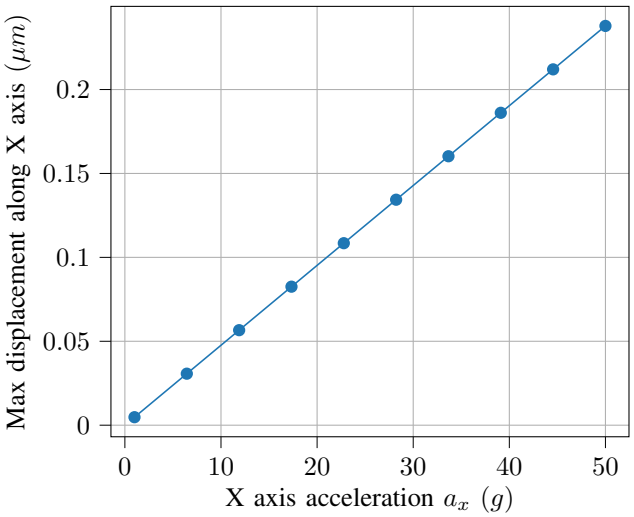

Fig. 13. Maximum displacement of the inertial mass along X axis for a_x accelerations between $1g$ and $50g$.

displacement plot, this is not true and the two segments and the junction move as well. This implies that the total equivalent x stiffness is obtained from the series of two springs: the straight beam, with spring constant equal to the k_x calculated in section II-B1, and the folded beam, with spring constant equal to the equivalent x stiffness of a folded beam structure. The fact that these springs are in series explains why the obtained stiffness is much smaller than the predicted one.

This x stiffness of the folded beam could be evaluated through analytical expressions, thanks to a more accurate model of the structure. However, this analysis goes beyond the scope of this report. On the other hand, it would be possible to retrieve an approximation of this stiffness value by using the inverse formula for springs in series:

$$k_{x,COMSOL} = \frac{k_{x,straight}k_{x,folded,tot}}{k_{x,straight} + k_{x,folded,tot}} \tag{20}$$

where $k_{x,straight} = 31.5335N/m$ is the total stiffness of the straight beams, $k_{x,COMSOL} = 17.1287N/m$ is the stiffness obtained with the simulation and $k_{x,folded,tot}$ is the total x stiffness of all the folded beams combined.

$$k_{x,folded,tot} = \frac{k_{x,COMSOL}k_{x,straight}}{k_{x,straight} - k_{x,COMSOL}} = 37.4964N/m \tag{21}$$

Therefore, the equivalent x stiffness of a single folded beam, supposing the four folded beams springs in parallel:

$$k_{x,folded} = \frac{k_{x,folded,tot}}{4} = 9.3741N/m \tag{22}$$

B. a_y parametric sweep

The 3D plots for this simulation are presented in figures 14, 15, 16 and 17.

The maximum displacements along the X axis of the inertial mass are listed in table V.

TABLE V
MAXIMUM Y DISPLACEMENT OF THE INERTIAL MASS FOR a_y ACCELERATIONS BETWEEN 1G AND 50G.

a_y [g]	Maximum Y displacement [μm]
1.0000	0.0024836
6.4444	0.016005
11.889	0.029527
17.333	0.043049
22.778	0.056571
28.222	0.070092
33.667	0.083614
39.111	0.097136
44.556	0.11066
50.000	0.12418

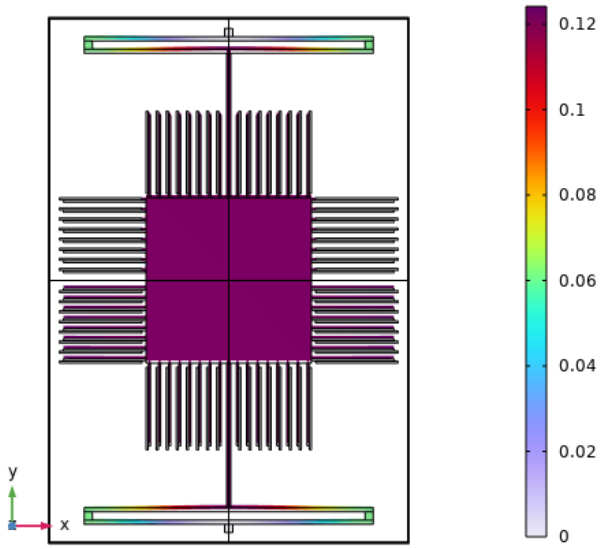

Fig. 14. Displacement (μm) for acceleration $a_y = 50g$.

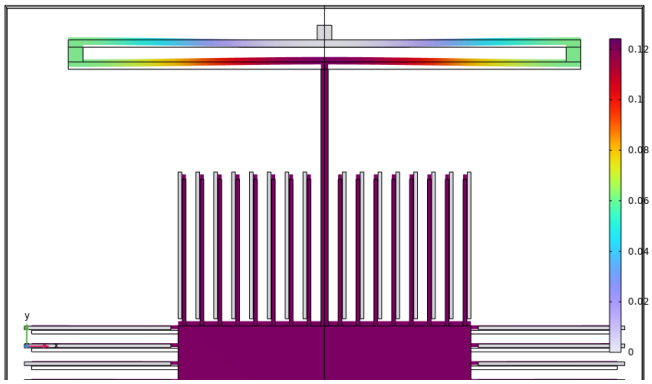

Fig. 15. Displacement (μm) for acceleration $a_y = 50g$, detail.

The maximum von Mises stress evaluated for different accelerations on the polysilicon structure is listed in table VI.

TABLE VI
MAXIMUM VON MISES STRESS OF THE POLYSILICON STRUCTURE FOR a_y ACCELERATIONS BETWEEN 1G AND 50G.

a_y [g]	Maximum Von Mises stress [MPa]
1.0000	0.052332
6.4444	0.33725
11.889	0.62217
17.333	0.90709
22.778	1.1920
28.222	1.4769
33.667	1.7618
39.111	2.0468
44.556	2.3317
50.000	2.6166

The maximum von Mises stress simulated for $a_y = 50g$ is $2.6166 \cdot 10^6 Pa$, which is almost identical to what is obtained in [2] ($2.5348 \cdot 10^6 Pa$). The same conclusions as before apply.

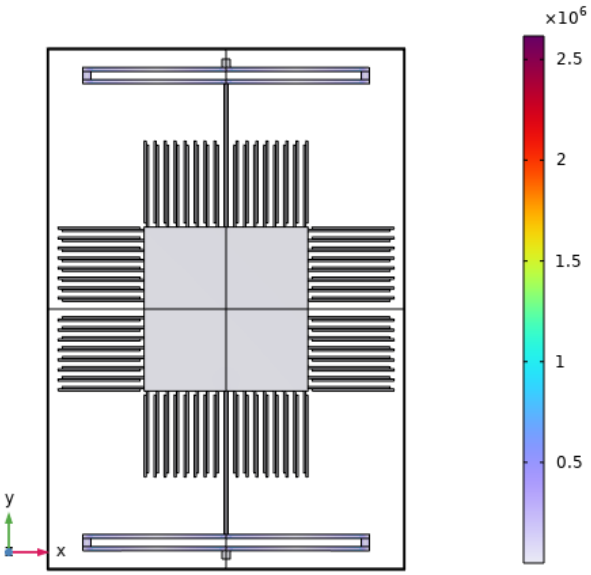

Fig. 16. Von Mises stress intensity (N/m^2) for acceleration $a_y = 50g$.

In figure 18 we can see that the relationship between the y displacement and the y acceleration (therefore, the force) is here as well quite linear, which means that the equivalent y stiffness is constant in the applied range of accelerations, as predicted by our model. The inverse of the mean slope of this curve multiplied by the total simulated inertial mass ($\frac{m}{8}$) gives us an equivalent y stiffness $k_{y,reduced} = 4.104 N/m$. Using equation 12, we obtain $k_y = 32.832 N/m$.

As explained in section II-B1, the y displacement sensitivity corresponds to the y displacement of the movable fingers for $a_y = 1g$. Considering the movable fingers as rigid bodies anchored to the central mass, we can evaluate the maximum displacement of the central mass, instead of the fingers'. The

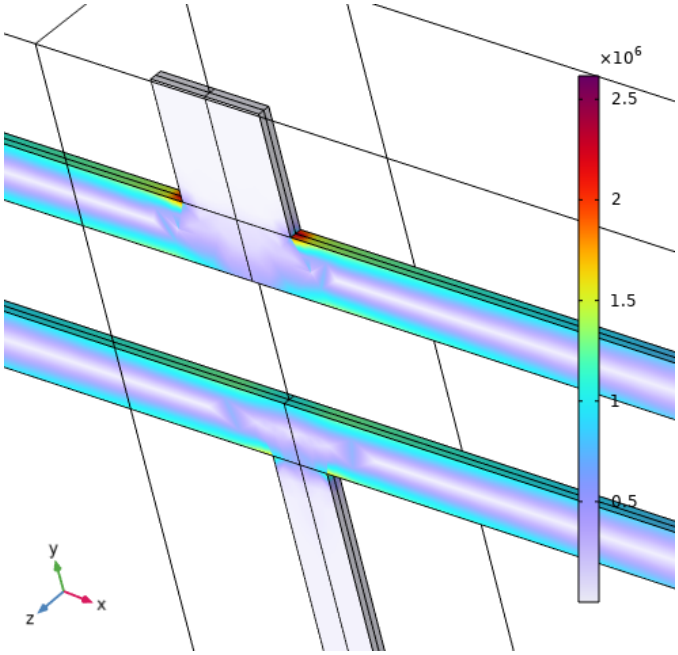

Fig. 17. Von Mises stress intensity (N/m^2) for acceleration $a_y = 50g$, detail of the folded beam attachment to the anchor.

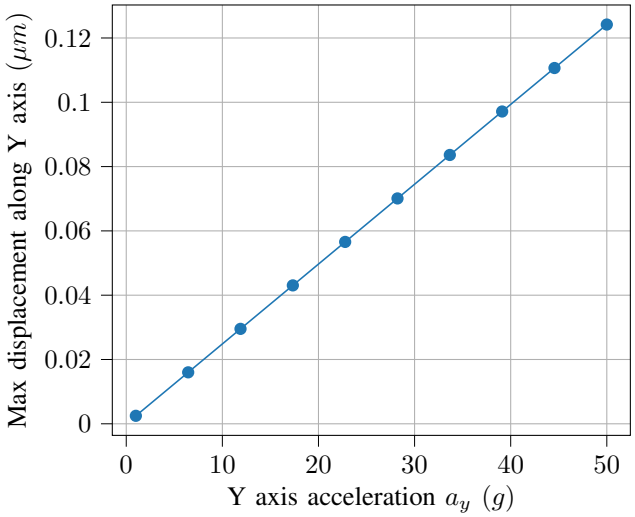

Fig. 18. Maximum displacement along Y axis for a_y accelerations between $1g$ and $50g$.

obtained sensitivity is $S_y = 0.0024836 \mu m$.

TABLE VII
COMPARISON OF SIMULATED AND THEORETICAL VALUES FOR THE Y EQUIVALENT STIFFNESS AND S_y SENSITIVITY.

Device Property	COMSOL	Theoretical
k_y [N/m]	32.832	31.5335
S_y [μm]	0.0024836	0.002587

Here, simulated results are quite similar to the predicted values, since no big approximation was made in the model of the Y springs.

C. t_{bx} parametric sweep

Through this simulation, it was possible to verify that the S_x sensitivity is inversely proportional to the thickness of the straight beam, as anticipated by equation 15.

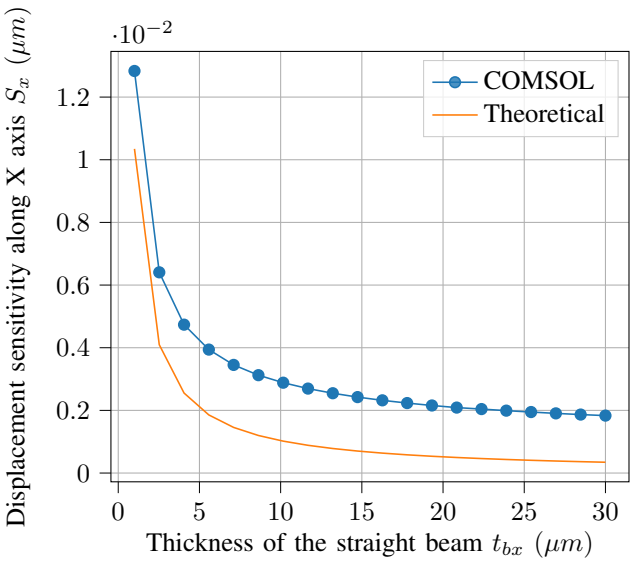

Fig. 19. Displacement sensitivity along X axis S_x for thicknesses of the straight beam t_{bx} between $1\mu m$ and $30\mu m$. The orange curve is the plot of equation 15 against t_{bx}.

A comparison between the theoretical and simulated values is presented in table VIII.

TABLE VIII
DISPLACEMENT SENSITIVITY ALONG X AXIS FOR DIFFERENT t_{bx} VALUES.

t_{bx} [μm]	**COMSOL** S_x [μm]	**Theoretical** S_x [μm]
1.0000	0.012833	0.01034695
2.5263	0.0064067	0.00409567
4.0526	0.0047361	0.00255314
5.5789	0.0039404	0.00185464
7.1053	0.0034515	0.00145624
8.6316	0.0031239	0.00119873
10.158	0.0028837	0.00101861
11.684	0.0026959	0.00088555
13.211	0.0025476	0.00078324
14.737	0.0024241	0.00070211
16.263	0.0023210	0.00063622
17.789	0.0022335	0.00058163
19.316	0.0021566	0.00053567
20.842	0.0020895	0.00049644
22.368	0.0020420	0.00046257
23.895	0.0019917	0.00043302
25.421	0.0019472	0.00040702
26.947	0.0019047	0.00038397
28.474	0.0018667	0.00036339
30.000	0.0018336	0.0003449

As already discussed in section IV-A, the theoretical model differs from the COMSOL simulation results because the equivalent x stiffness of the folded beams was not considered for simplicity. It is possible to compare the relative errors made for the x displacement sensitivity evaluation between the COMSOL simulation and the theoretical model with and without this approximation. The analytical expression for the displacement sensitivity considering the x stiffness of the folded beams can be obtained from equation 15, replacing k_x with 20, where $k_{x,folded,tot}$ is evaluated in equation 21. The result is shown in figure 20. The theoretical adjusted sensitivity values can be found in table IX.

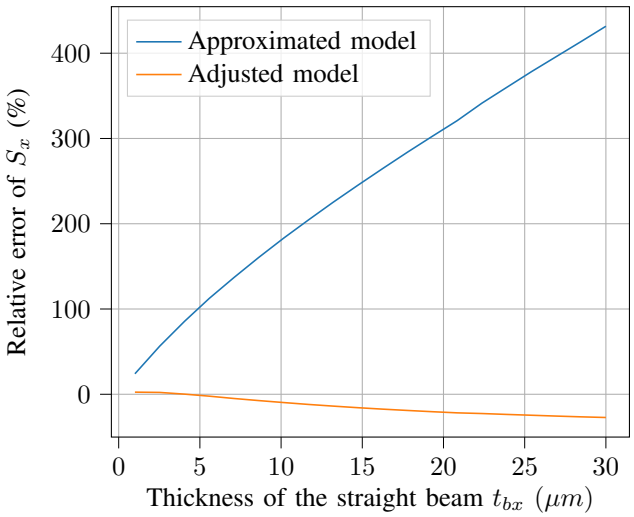

Fig. 20. Relative error of S_x between the COMSOL simulation and the theoretical model with and without approximation on the stiffness of the folded beams.

TABLE IX
DISPLACEMENT SENSITIVITY ALONG X AXIS FOR DIFFERENT t_{bx} VALUES. ADJUSTED MODEL INCLUSIVE OF FOLDED BEAMS X STIFFNESS.

t_{bx} [μm]	**COMSOL** S_x [μm]	**Theoretical adjusted** S_x [μm]
1.0000	0.012833	0.01252233
2.5263	0.0064067	0.00627105
4.0526	0.0047361	0.00472853
5.5789	0.0039404	0.00403002
7.1053	0.0034515	0.00363162
8.6316	0.0031239	0.00337411
10.158	0.0028837	0.00319399
11.684	0.0026959	0.00306093
13.211	0.0025476	0.00295862
14.737	0.0024241	0.0028775
16.263	0.0023210	0.0028116
17.789	0.0022335	0.00275702
19.316	0.0021566	0.00271106
20.842	0.0020895	0.00267183
22.368	0.0020420	0.00263795
23.895	0.0019917	0.0026084
25.421	0.0019472	0.00258241
26.947	0.0019047	0.00255935
28.474	0.0018667	0.00253877
30.000	0.0018336	0.00252028

D. w_{bx} parametric sweep

Through this simulation, it was possible to verify that the S_x sensitivity is inversely proportional to the cubic power of the width of the straight beam, as anticipated by equation 15.

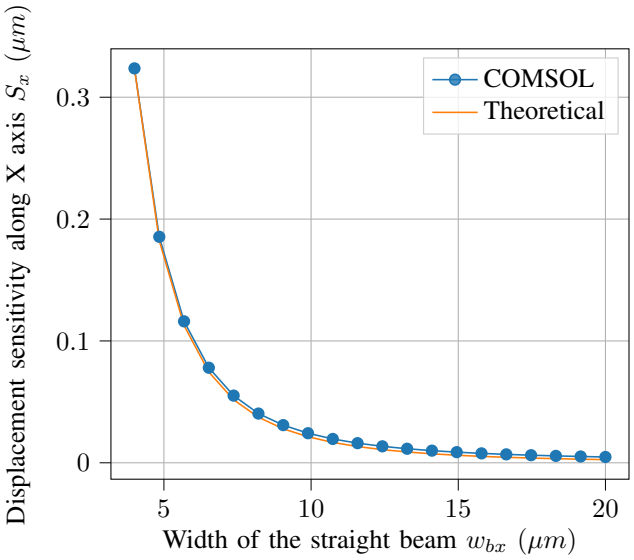

Fig. 21. Displacement sensitivity along X axis S_x for thicknesses of the straight beam w_{bx} between $4\mu m$ and $20\mu m$. The orange curve is the plot of equation 15 against w_{bx}.

A comparison between the theoretical and simulated values is presented in table X.

TABLE X
DISPLACEMENT SENSITIVITY ALONG X AXIS FOR DIFFERENT w_{bx} VALUES.

w_{bx} [μm]	**COMSOL** S_x [μm]	**Theoretical** S_x [μm]
4.0000	0.32367	0.32334224
4.8421	0.18546	0.1822803
5.6842	0.11608	0.11267614
6.5263	0.078004	0.07444545
7.3684	0.055130	0.05172722
8.2105	0.040408	0.03738776
9.0526	0.030917	0.02789446
9.8947	0.024271	0.0213614
10.737	0.019561	0.01671909
11.579	0.016106	0.01333015
12.421	0.013517	0.01079859
13.263	0.011525	0.00886955
14.105	0.0099635	0.00737393
14.947	0.0087316	0.00619652
15.789	0.0077321	0.00525702
16.632	0.0069123	0.00449823
17.474	0.0062323	0.00387872
18.316	0.0056619	0.00336795
19.158	0.0051798	0.00294306
20.000	0.0047630	0.00258674

Conclusions analogous to the ones of the previous study can be drawn. The model can be adjusted by considering the equivalent x stiffness of the folded beams. The improvement obtained in the relative error made in the evaluation of the x displacement sensitivity is shown in figure 22. The new adjusted values are listed in table XI.

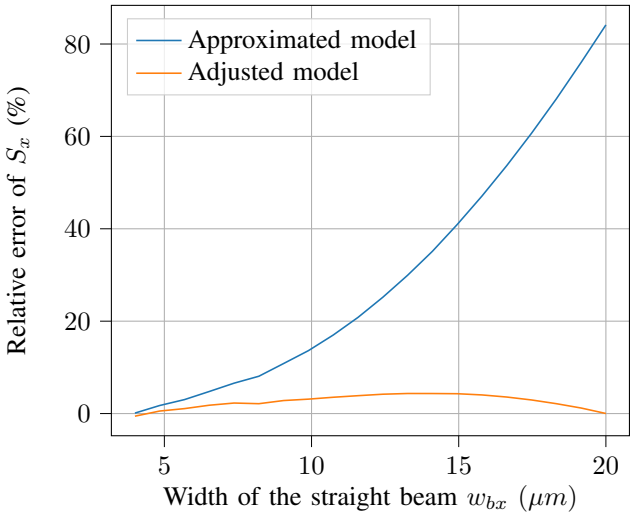

Fig. 22. Relative error of S_x between the COMSOL simulation and the theoretical model with and without approximation on the stiffness of the folded beams.

TABLE XI
DISPLACEMENT SENSITIVITY ALONG X AXIS FOR DIFFERENT w_{bx} VALUES. ADJUSTED MODEL INCLUSIVE OF FOLDED BEAMS X STIFFNESS.

w_{bx} [μm]	**COMSOL** S_x [μm]	**Theoretical adjusted** S_x [μm]
4.0000	0.32367	0.32551763
4.8421	0.18546	0.18445569
5.6842	0.11608	0.11485152
6.5263	0.078004	0.07662083
7.3684	0.055130	0.0539026
8.2105	0.040408	0.03956314
9.0526	0.030917	0.03006984
9.8947	0.024271	0.02353678
10.737	0.019561	0.01889448
11.579	0.016106	0.01550554
12.421	0.013517	0.01297398
13.263	0.011525	0.01104493
14.105	0.0099635	0.00954931
14.947	0.0087316	0.00837191
15.789	0.0077321	0.0074324
16.632	0.0069123	0.00667362
17.474	0.0062323	0.00605411
18.316	0.0056619	0.00554333
19.158	0.0051798	0.00511844
20.000	0.0047630	0.00476212

V. CONCLUSIONS

The obtained results are coherent with the reference paper, from which the design idea of this dual-axis accelerometer was taken [2]. In particular, the maximum stress of the polysilicon structure and the displacement sensitivities to input accelerations present negligible differences.

However, the theoretical model proposed in [2] is not very accurate for the prediction of the device stiffness along X axis, due to approximating the x stiffness of the folded beams as

infinite, which turns out not to be true. Adjustments were made in order to compensate for this error. Nevertheless, the approximated model effectively managed to predict the dependency of the displacement sensitivity S_x as a function of the straight beam thickness t_{bx} and width w_{bx}. This result can be helpful in the design and optimization of dual-axis accelerometers with T-shape beams.

REFERENCES

[1] Hergen Kapels, Robert Aigner, and Josef Binder. "Fracture strength and fatigue of polysilicon determined by a novel thermal actuator [MEMS]". In: *Electron Devices, IEEE Transactions on* 47 (Aug. 2000), pp. 1522 –1528. DOI: 10.1109/16.848302.

[2] Ce Zheng, Xingguo Xiong, and Junling Hu. "COMSOL Simulation of a Dual-axis MEMS Accelerometer with T-shape Beams". In: Oct. 2015.